

Enhanced group V intermixing in InGaAs/ InP quantum wells studied by cross- sectional scanning tunneling microscopy

Huajie Chen and R.M. Feenstra

Department of Physics, Carnegie Mellon University, Pittsburgh, Pennsylvania
15213

P.G. Piva, R.D. Goldberg and I.V. Mitchell

Department of Physics and Astronomy, University of Western Ontario, London
N6A3K7, Canada

G.C.Aers, P.J. Poole and S. Charbonneau

Institute for Microstructural Sciences, National Research Council of
Canada, Ottawa, Canada K1A0R6

Abstract

Cross-sectional scanning tunneling microscopy is used to study InGaAs/
InP quantum well intermixing produced by phosphorus implantation.
When phosphorus ions are implanted in a cap layer in front of the quantum
wells (in contrast to earlier work involving implantation through the
wells), clear strain development is observed at the interfaces between
quantum well and barrier layers after annealing. This is interpreted in
terms of enhanced group V compared to group III interdiffusion.

Interdiffusion of quantum well (QW) structures[1] has recently been investigated as a
means of integrating regions of different band gap in the same epitaxial layer for photonic integrat-
ed device applications.[2] However, greater knowledge of the microscopic mechanisms of QW in-
termixing is required to optimize this process. Techniques used to study QW intermixing include
transmission electron microscopy (TEM), photoluminescence (PL) and X-ray diffraction (XRD).
In a previous study we demonstrated that scanning tunneling microscopy (STM) images can clear-
ly show the amount of intermixing by observing the QW width change.[3] In this paper, STM is
shown to be capable of observing the strain development after intermixing. Such strain variation
can be exploited in applications such as polarization-independent amplifiers, where the strain leads
to the convergence of heavy and light hole absorption edges.[4]

In our study, an InGaAs/InP multiple quantum well (MQW) structure is used. Implantation
of P ions produces a large concentration of defects, which enhance the interdiffusion during sub-
sequent annealing. In our previous study,[3] the samples had a thin InP cap layer and P ions were
implanted *through* the MQW stack. No evidence of strain development was observed in that case
which suggests that group V (anion) and group III (cation) atoms intermix at similar rates. In this
study, P ions are implanted into a thick cap layer in front of the MQW stack. Contrary to the pre-
vious results,[3] significant strain development is observed across the QW structure. With the use
of finite element modeling, the strain development is attributed to a group V to group III interdif-

fusion length ratio of about 1.7.

The sample used in this study was grown by Chemical Beam Epitaxy (CBE). It consists of a 20 period stack of 6 nm nominally lattice-matched $\text{In}_{0.53}\text{Ga}_{0.47}\text{As}$ QWs with 18 nm InP barriers, and capped with 1.56 μm of InP. The structure was doped n-type with silicon to a level of $2 \times 10^{17} \text{cm}^{-3}$. Samples were implanted with 500 keV phosphorus ions, at a substrate temperature of 200°C and 7° off-normal to minimize ion channeling. This implantation energy ensured that the range of the implanted ions was much less than the location of the first InGaAs QW, 1.56 μm beneath the surface. Ion flux and fluence were 26 nA cm^{-2} and $1 \times 10^{14} \text{ ions cm}^{-2}$ respectively. For the STM images shown here, the samples were given a rapid thermal anneal (RTA) at 675°C , for 90 s. No significant PL blue shift resulted, thus necessitating a second RTA, for 90 s at 725°C . Low temperature (4.2K) PL measurements give a blue shift of 110 meV for the implant+RTA sample, relative to the as-grown MQW PL energy, while only a 10 meV blue shift is observed for the RTA-only sample. STM images obtained from samples undergoing a single 90 s 740°C RTA are similar to those reported here, albeit having lower resolution due to a blunter probe tip.

The experimental arrangement of the STM was identical to that described previously.[3] STM images are shown in Fig. 1, each image displaying one quantum well of the 20 period MQW stack. The InGaAs layers appear as the mottled black and white region in the center of each image, their appearance arising from fluctuations in alloy composition. Fig. 1(a) shows the as-grown sample, with a well width of 6.0 nm. The sample after ion implantation/RTA is shown in Fig. 1(b). Implantation enhanced intermixing between the InGaAs and InP layers is clearly seen, with the width of alloy layer increasing to about 7.9 nm. STM observation of different QWs in the 20 period MQW stack shows similar intermixing throughout the structure. This indicates that point defects can diffuse through 0.48 μm of MQW material without significant trapping, and that the 40 InGaAs/InP interfaces have no obvious effect on the defect transport.

As clearly seen in Fig. 1(b), a white band appears near the well/barrier interface after intermixing. This white contrast (higher tip height) is seen for both positive and negative STM sample voltages. STM line scans, averaged over the images of Figs. 1(a) and (b), are shown in (c) and (d) respectively. In such constant current images, the tip height variation can come from sample topographical variation or electronic effects. As discussed below, the electronic effect for the InGaAsP system with sample voltage of $\gtrsim 2 \text{ V}$ is small, so the observed tip height variation mainly comes from a surface topographical variation. Since the cleavage face is clearly free of steps, we attribute the observed topographic variation to strain relaxation of the underlying materials, with compressively strained regions protruding outwards and tensilely strained regions contracting inwards.[5] For the as-grown sample, some variation in topography occurs [Fig. 1(c)], which arises from several sources: First, in the InP barrier overgrown on the InGaAs well, arsenic carryover occurs as marked in Fig. 1(a), and this produces compressive strain giving rise to an increasing topography as one approaches the quantum well. On the other side of the well, a discontinuity of about 0.1 \AA in height is seen between the well and the barrier. This topographic change presumably arises from some small net strain between well and barrier, together with possible small electronic effects in the image contrast. Finally, the small increase in topography (protrusion) seen on the right hand side of the quantum well arises from an apparent concentration of In-rich clusters in the well, which are reproducibly observed on the right hand side of all the as-grown well layers.

In contrast to the as-grown material, the intermixed material shown in Fig. 1(d) displays a large surface undulation, with the center of the well being tensilely strained and the interfaces between well and barrier being compressively strained. For the data of Fig. 1(d) the observed topographic variation is relatively symmetric across the quantum well, but in other cases (particularly near the top of the QW stack) we find a significantly larger topographic height for the barrier-on-well interface compared to the well-on-barrier interface. By modeling the observed strain variations of Fig. 1, we can obtain a semi-quantitative measure of the group III and V interdiffusion lengths, as shown in Figs. 2 and 3. We assume an error function form for the interdiffusion profiles, characterized by interdiffusion lengths Δ_{III} and Δ_V . [6] For a given choice of these parameters, finite element modeling is used to compute the height variation of the cleaved surface arising from the strain in the underlying layers. Results are shown in Figs. 2(a) and (b), with the corresponding composition profiles shown in (c) and (d) respectively. In terms of the ratio $K \equiv \Delta_V / \Delta_{III}$, we find that for $K > 1$ [Fig. 2(a)] the surface height resembles that observed experimentally with protrusions near the quantum well edges, whereas for $K < 1$ the height variations are inverted [Fig. 2(b)]. Thus, the STM images directly yield the nature of the diffusion asymmetry, *i.e.* $\Delta_V > \Delta_{III}$.

We justify our neglect of possible electronic contributions to the STM images by an explicit computation of band structure (using nonlocal pseudopotentials) and tunnel current [7] for the InGaAsP quaternary system, as discussed in detail elsewhere. [8] The tunnel current is very insensitive to band structure details, particularly for energies (voltages) > 2 eV above the band edges. (Surface state effects are neglected, consistent with tunneling spectroscopy results which show them to have only a small effect on the current. [9]) We find that, for sample voltages > 2 V above the band edges, there is at most a factor of 2 variation in the tunnel current among the GaAs, InAs, GaP, and InP materials, corresponding to a tip height variation of < 0.3 Å. For the restricted range of alloy compositions occurring in the intermixed quantum wells [Figs. 2(c) and (d)], the expected size of electronic effects is smaller, being < 0.1 Å. We conclude that, to first order, electronic contributions to the images can be neglected.

Group III and group V interdiffusion lengths are determined as shown in Fig. 3. Contours of constant undulation amplitude A are displayed [positive A are for undulations with shape as in Fig. 2(c), and negative A are as in Fig. 2(d)]. Experimentally, we find an amplitude of about 0.4 Å, which then determines a set of allowable values for Δ_{III} and Δ_V . A unique determination of the interdiffusion lengths can be accomplished using additional information obtained from the observed PL shift of 110 meV. Values of Δ_{III} and Δ_V which yield this value of the PL shift [6] are shown as the solid line in Fig. 3. We thereby deduce values of $\Delta_V \sim 1.4$ nm and $\Delta_V / \Delta_{III} \sim 1.7$.

The preferred group V interdiffusion observed here is confirmed by XRD measurements. Significant strain development is observed in the (004) XRD scans of the intermixed sample when compared to the as-grown, with the intensity of the x-ray satellite peaks increasing by an order of magnitude after intermixing. This result can only be explained by an increase in the strain modulation through the structure, [10] consistent with the STM result. We note that an advantage of the STM analysis compared to that of XRD is that it permits a simple, direct determination of the sign of the diffusion asymmetry.

The results described above are in contrast with our previous study [3a], in which ions were

implanted *through* the MQW stack and where no evidence was found of different group III and V interdiffusion rates after intermixing.[11] After implantation through the QWs, both group III and V point defects are available in the MQW region and it is possible to intermix both sublattices roughly equally. However, in the present study, ions are implanted short of the MQW stack and point defect transportation is required over long distances to reach the QWs. In this case, any greater supply of defects which promote group V interdiffusion will lead to the observed effects. For example, the implantation species (P) or the emission mechanism of mobile defects from the complex damage region may tend to increase the supply of defects which produce group V interdiffusion.[12]. Alternatively, different mobility in the cap layer of defects causing group III and V interdiffusion could also contribute to the observed effects. Additional experiments, utilizing indium ions for implantation, are underway in an effort to identify the relevant mechanism(s).

We thank C. Lacelle for technical assistance with CBE growth, and gratefully acknowledge M. Fischetti for providing the band structure program used here. This work was supported by grants from NSERC and NSF.

- [1] See for example, D. G. Deppe and N. Holonyak Jr., J. Appl. Phys. **64**, R93 (1988).
- [2] S. Charbonneau *et al.*, J. Appl. Phys. **78**, 3697 (1995).
- [3] P.G. Piva *et al.*, Appl. Phys. Lett. **72**, 1599 (1998).
- [4] J.-J. He, S. Charbonneau, P.J. Poole, G.C. Aers, Y. Feng, E.S. Koteles, R.D. Goldberg and I.V. Mitchell, Appl. Phys. Lett. **69**, 562 (1996).
- [5] H. Chen, R. M. Feenstra, R. S. Goldman, C. Silfvenius, and G. Landgren, Appl. Phys. Lett. **72**, 1727 (1998).
- [6] J. Micallef, E.H. Li, and B.L. Weiss, J. Appl. Phys. **73**, 7524 (1993).
- [7] C. B. Duke, *Tunneling in Solids* (Academic, New York, 1969), Eq. (7.8b).
- [8] R. M. Feenstra and H. Chen, to be published.
- [9] R. M. Feenstra, Phys. Rev. B **50**, 4561 (1994).
- [10] S.-W. Ryu, B.-D. Choe, and W. G. Jeong, Appl. Phys. Lett. **71**, 1670 (1997).
- [11] Since the Si doping level in the present sample is substantially lower than in the previous study[3] ($2 \times 10^{17} \text{ cm}^{-3}$ compared to $8 \times 10^{18} \text{ cm}^{-3}$), we also implanted *through* the MQW region of the present sample with 4.7 MeV P ions and found very little strain development from XRD/STM, similar to our first STM study.[3]
- [12] E.g., in analogy to proposed processes in silicon: M. D. Giles, J. Electrochem. Soc. **138**, 1160 (1991); D.J. Eaglesham, P.A. Stolk, H.-J. Gossmann, and J.M. Poate, Appl. Phys. Lett. **65**, 2305 (1994); L. Pelaz *et al.*, Appl. Phys. Lett. **73**, 1421 (1998).

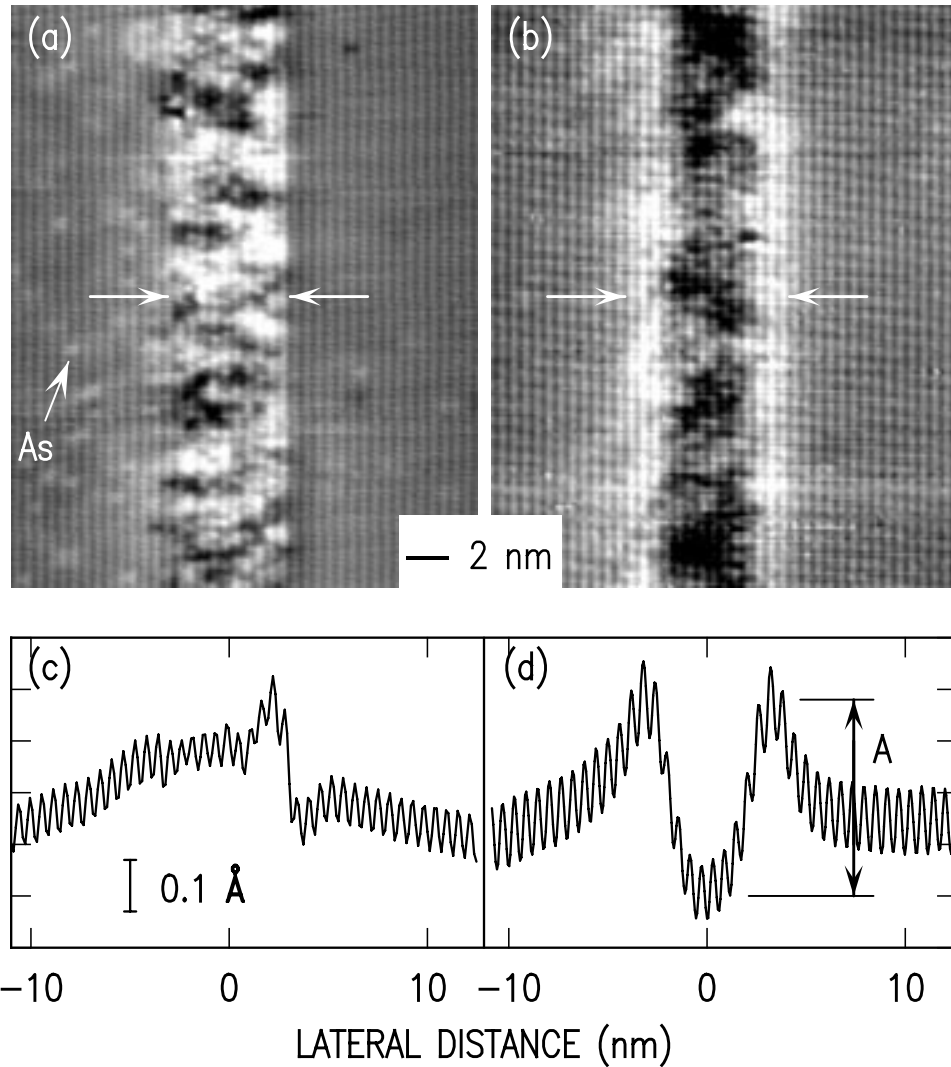


Figure 1 Cross-sectional STM images of InGaAs/InP heterostructures, (a) as-grown sample; (b) implant+RTA sample. Images were acquired at sample voltages of +2.5 and +2.0 V respectively, and grey scale ranges are 0.05 and 0.06 nm respectively. The symbol As in panel (a) indicates one of many arsenic atoms which appear as faint white features in the InP barrier layer. An average of the topographic line scans is shown in (c) and (d), with the undulation amplitude A indicated in (d). Layer growth direction is from right to left. Arrows indicate approximate width of the quantum wells.

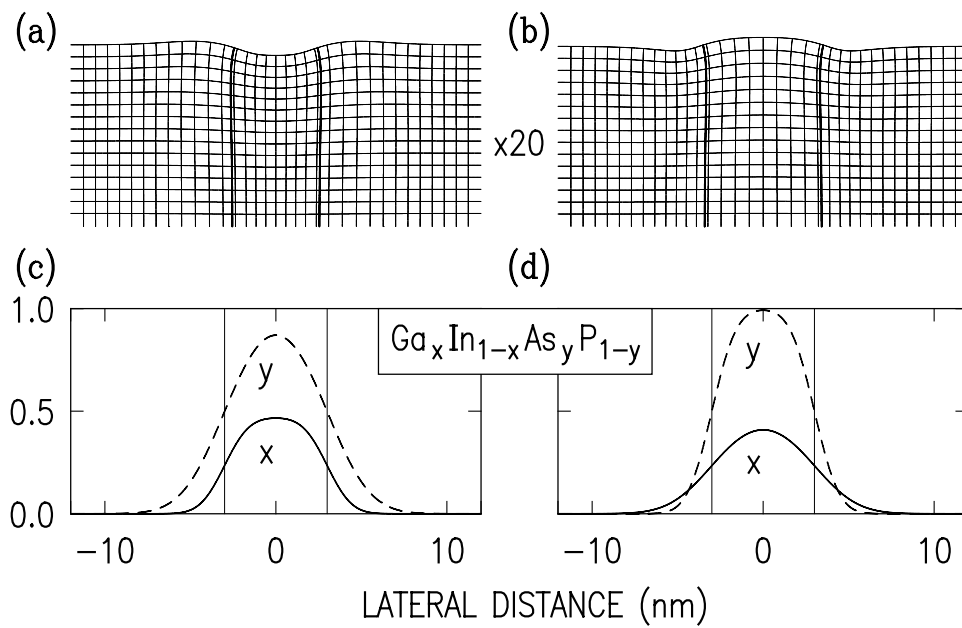


Figure 2 (a) and (b) Cross-sectional view of heterostructure, showing results of finite element computations for the displacement of lattice planes (multiplied by 20, for clarity). Composition profiles used in (a) and (b) are shown in (c) and (d), respectively. Profiles are generated using group III/V interdiffusion lengths of (c) 0.8 nm/1.4 nm, and (d) 1.4 nm/0.8 nm, respectively.

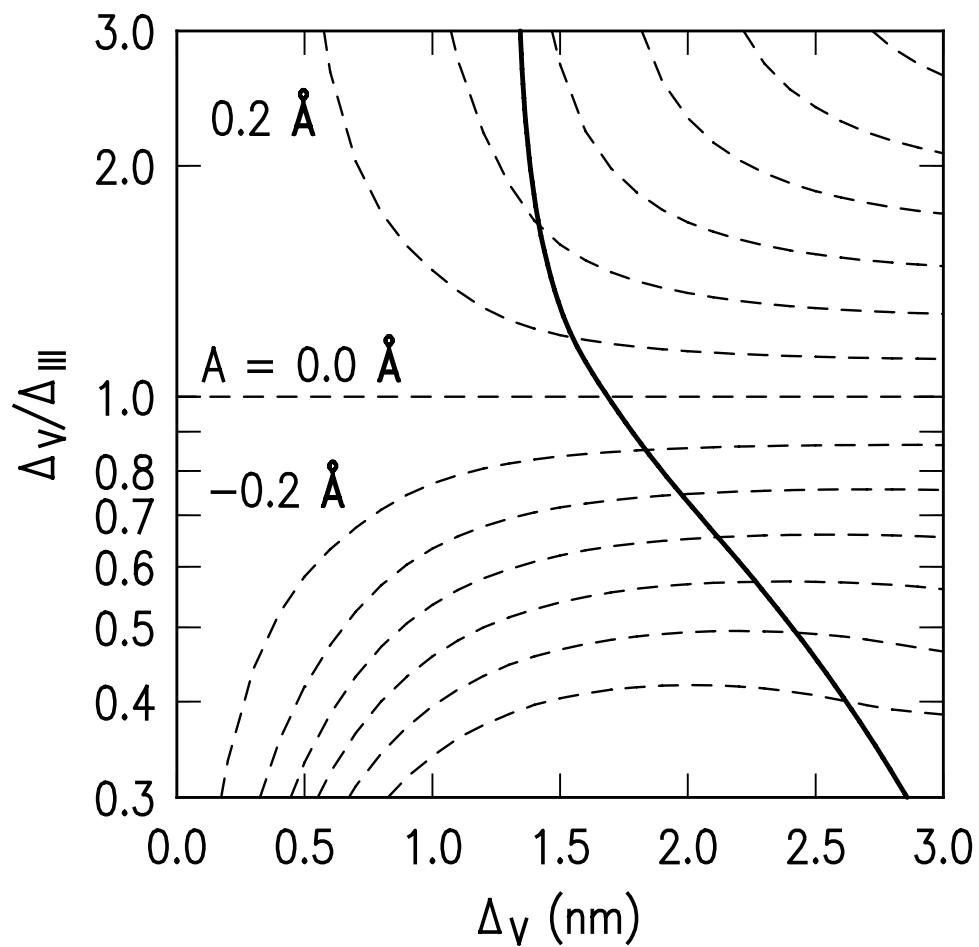


Figure 3 Dashed line show contours of constant undulation amplitude A , spaced by 0.2 \AA as indicated, as a function of group V interdiffusion length Δ_V , and group V to III interdiffusion length ratio Δ_V/Δ_{III} . The thick solid line shows the interdiffusion lengths which produce a PL shift of 110 meV.